UAV Icing: A Survey of Recent Developments in Ice Detection Methods ⋆

Bogdan Løw-Hansen [*,**] **Richard Hann** [*,**]
Bård Nagy Stovner [**] **Tor Arne Johansen** [*]

[*] *Dep. of Engineering Cybernetics, NTNU, Trondheim, Norway, (e-mail: {bogdan.l.hansen, richard.hann, tor.arne.johansen}@ntnu.no)*
[**] *UBIQ Aerospace, 7011, Trondheim, Norway, (e-mail: bard.stovner@ubiqaerospace.com)*

Abstract: In-flight icing remains a significant challenge for the aviation industry. While mature solutions for conventional aircraft exist, the options for small fixed-wing uncrewed aerial vehicles (UAVs) are limited, with the current solution being to postpone the flight until icing conditions have passed. Consequently, the challenges related to aircraft icing continue to be highly relevant, but now with a stronger emphasis on size, cost, and efficiency to better fit the smaller UAV platforms, which are currently experiencing high commercial interest. A crucial prerequisite for efficient ice protection solutions is the availability of real-time ice detection systems. This survey aims to provide an overview of recent developments in research on in-flight icing detection solutions suitable for UAVs. The survey covers atmospheric icing detection, direct ice detection, and indirect ice detection methods. Among these, the indirect methods, which are based on monitoring the aircraft performance degradation due to in-flight icing, are emphasized. The performance-based methods rely on flight data analysis, estimation, and detection algorithms, making them ideal for UAVs as they require only minimal aircraft modification and can be implemented retrospectively.

Keywords: UAVs; decision making, autonomy, sensor data fusion; health monitoring, diagnosis

NOMENCLATURE

h	Altitude
u, v, w	Body frame velocities
p, q, r	Roll, Pitch, Yaw angle rates
ϕ, θ, ψ	Roll, Pitch, Yaw angles
α	Angle of attack
β	Sideslip
ψ_w	Horizontal wind direction
V_a	Horizontal airspeed
V_g	Ground speed
V_w	Wind speed
V_{sw}, V_{dw}	Static and dynamic wind components
ω	Motor shaft speed
i	Motor current
T	Motor thrust
Q	Motor torque
λ	Pitote tube measurement scale factor
$\bar{q}$	Trim dynamic pressure
η_{ice}	Icing factor
K_{C_*}	Coefficient specific icing factor
C_*	Nominal coefficients and derivatives
$C_*^\star$	Iced coefficients and derivatives
X, Y, Z	Body frame forces
l, m, n	Body frame moments
L, D, N	Lift, drag and normal forces
$\delta_a, \delta_e, \delta_{th}$	Aileron, elevator and throttle control inputs
I_{xx}, I_{yy}, I_{zz}	Diagonal moments of inertia
g	Gravitational acceleration
P	Vector of parameters to be estimated
m	Mass of the aircraft
S	Wing surface area
μ_*	Aircraft specific factor
γ	Hypothesis test threshold
t	Time
$_k$	Discrete time index
$_0$	Trim condition subscript
$_*$	Variable placeholder
$\hat{}$	Indicator for estimated variable or parameter

1. INTRODUCTION

One of the significant challenges in the aviation industry is the operation of uncrewed aerial vehicles (UAVs) in adverse weather conditions, where icing is considered especially problematic (Hann and Johansen, 2020).

On conventional aircraft, the challenges related to icing have been addressed by deploying relatively expensive ice detection sensors and ice protection systems, which often require significant amounts of energy to operate (Deiler and Fezans, 2020). The same approach cannot be readily applied to UAVs, which operate under different operational and logistical constraints. The limiting factors for implementing conventional aircraft solutions on UAVs are the cost, weight, and efficiency constraints. However, due to the rapid adoption of UAVs, finding solutions that respect these constraints has become highly relevant, leading

⋆ The work is partly sponsored by the Research Council of Norway through the Center of Excellence funding scheme, project number 223254, AMOS, and IKTPLUSS project number 316425.

to a substantial increase in ice detection research, which is surveyed in this paper. The increased interest in UAVs can be observed in market analysis reports as well. According to Markets and Markets (2018) report, the commercial UAV market was projected to increase sixfold from 2018 to 2025, and according to Federal Aviation Administration (2022) report, the current commercial UAV fleet in the United States will increase by 38% by 2026. The increased academic and commercial interest in UAVs has enabled a new wave of UAV-related research, including research on in-flight icing detection, clearly visualized by Fig. 1.

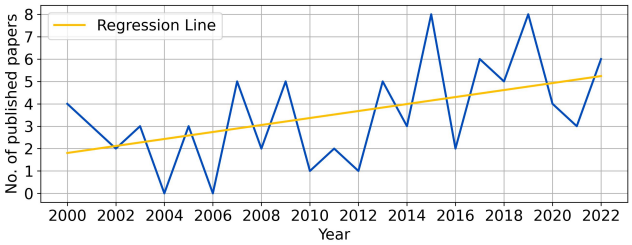

Fig. 1. Number of published papers per year on the topic of in-flight icing detection in the period 2000-2022. Data is based on articles surveyed in this paper.

In conventional aviation, there are several methods to tackle in-flight icing. Popular approaches in conventional aviation include chemical solutions — freezing point depressant fluids applied to the airframe before takeoff, deicing boots — a pneumatic system that inflates the boot to break off accreted ice — and continuous heating of aircraft lifting surfaces by bleed air systems during icing conditions. However, these solutions have some drawbacks. They are costly, non-scalable, or increase the aircraft's weight, making them unsuitable for most UAVs.

The effectiveness of any active ice protection system depends on the system's ability to detect ice. Therefore, in-flight icing detection is a critical stepping stone in addressing UAV icing. Based on the survey's results, there are mainly three approaches that researchers have taken:

- **Atmospheric icing detection** — detection of icing conditions, i.e., the presence of supercooled liquid droplets in the atmosphere.
- **Direct ice detection** — detection of ice accretion on the body of the aircraft.
- **Indirect ice detection** — inference of ice accretion based on the change in performance of the aircraft.

In theory, the detection methods for in-flight icing that were developed for conventional aviation can also be utilized for smaller fixed-wing UAVs. This is because the physical process of ice accretion and its effects on the aircraft are similar in both cases (Hann and Johansen, 2021). As a result, it has been deemed pertinent to survey the methods used for both aircraft types. Based on similar reasoning, the research on rotorcraft is excluded from this survey, as solutions developed for rotorcraft are often not applicable to fixed-wing UAVs.

During the preparation work for this survey, it was registered that there are only two major reviews on in-flight icing detection. A review by Jackson and Goldberg (2007), and a review by Caliskan and Hajiyev (2013), both written prior to the recent upsurge in UAV-based research. As such, this survey aims to highlight the recent developments in in-flight icing detection methods developed for UAVs. The main focus of this survey is on performance-based methods as they require minimal modification to the aircraft and can be implemented retrospectively, making them especially suitable for small fixed-wing UAVs.

2. REVIEW METHODOLOGY

This survey is based on 81 articles from 2000-2022 on the topic of aircraft icing detection, 57 of the articles concern aircraft in general, while the remaining 24 focus specifically on UAVs.

The databases that were used to find the articles are Scopus and Google Scholar. According to Martín-Martín et al. (2021), the combined results of these two databases should cover most of the published research work.

As stated in the introduction, this survey focuses on ice detection solutions applicable to conventional aircraft and smaller fixed-wing UAVs. Thus, detection techniques for jet engine icing and solutions designed for rotorcraft were excluded. To achieve the specified topic selection, specific keywords were utilized to narrow down the search space for the survey. The search included phrases "in-flight" AND ("ice detection" OR "icing detection"), along with at least one of the words from the list "aircraft," "UAV," "UAS," "VTOL," "drone," where the terms (UAS) and (VTOL) refer to unmanned aerial systems and vertical take-off and landing, respectively. Keywords such as "wind turbine," "multirotor," "rotorcraft," "turbofan," "ground-based," and "certification" were excluded from the search results. Additionally, to focus on recent developments, only articles published after 1999 were considered.

This survey has a limitation in that it only includes English-written articles. While English is the dominant language for research, some relevant research may have been published in other languages. To provide more context, a visualization of the distribution of papers by country of origin is presented in Fig. 2. It is worth noting that this limitation may result in an underrepresentation of research from certain countries, such as China, where a significant amount of research is published in Chinese.

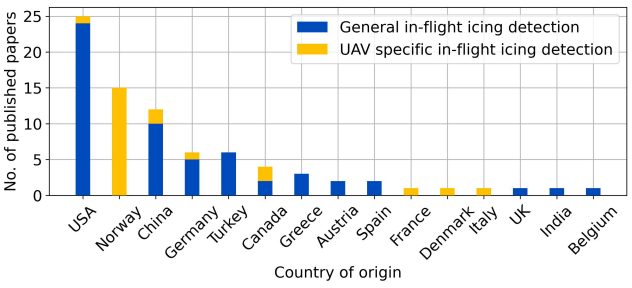

Fig. 2. Number of published papers by country of origin on in-flight icing detection in the period 2000-2022. The bar chart is based on data included in this survey.

3. DIRECT ICE DETECTION

In this section, the direct ice detection methods, which try to solve the problem by sensing the presence of ice on the wings and the body of the aircraft, are presented.

Many of the methods presented here are described in greater detail in (Jackson and Goldberg, 2007). Nevertheless, several newer articles demonstrating direct ice detection solutions are included in the present article.

3.1 Impedance and Capacitance Sensor

The primary ice detection method used in conventional aircraft is based on impedance and capacitance sensors. These methods work based on the following principle — when two electrodes are placed near each other and excited with alternating current, an impedance can be measured depending on the material between the electrodes. If, for instance, such electrodes are mounted on the surface of an aircraft, the measured impedance will vary if there is ice, water, or just air between the electrodes, thus making it possible to detect ice. A production-ready ice sensing solution based on impedance measurement is presented in (Botura and Fahrner, 2003). More recently, Schlegl et al. (2019) tested a similar impedance-based solution originally designed for wind turbines. Their results indicate that the solution has the potential to be useful. However, current thresholds tuned for wind turbines are unsuitable for aircraft applications. Several articles presenting impedance- and the closely related capacitance-based ice detection sensors are listed here (Roy et al., 2000; Jarvinen, 2007; Schlegl et al., 2015; Xie et al., 2022b; Zheng et al., 2022).

3.2 Vibration Probe Sensor

Similarly to impedance sensors, vibrations probe sensors are also a standard solution used in conventional aircraft. The idea of using a vibration probe as an ice detection sensor is based on the change in the neutral frequency of the vibration as ice mass accretes on the probe. In practice, this can be achieved by using magneto-restrictive coils and a probe made of ferromagnetic materials. Through excitation by alternating current, the magneto-restrictive coils can make the ferromagnetic probe expand and contract at its natural frequency. As the mass of the probe changes, so does the natural frequency of its vibration, making it possible to detect ice (Jackson and Goldberg, 2007). Similar ice-detection solutions based on high-frequency vibration measurements can be found in the following articles (Fuleki et al., 2017; Mäder et al., 2018; Xie et al., 2022a; Sohail et al., 2022).

3.3 Heat of Fusion Sensor

The rate of temperature change in a thin wire subjected to electric pulses can be used to detect the presence of ice around the wire. The idea relies on the fact that when an electric pulse is sent through a wire surrounded by ice, the generated heat will be used in the fusion process, changing the state of ice from solid to liquid instead of increasing the temperature of the ice. The lack of temperature increase during an electric pulse can therefore be interpreted as a build-up of ice around the wire (Jackson and Goldberg, 2007). A similar method is also investigated in the context of UAV icing by Hann et al. (2019) and by Sørensen and Johansen (2017), where an electrothermal ice detection system is tested in UAV flight tests.

3.4 Rotating Wheel Torque Sensor

A rotating wheel can be used in an ice detection system by fulfilling two functions — torque measurement and ice collection. When ice accretes on the rotating wheel, it widens its diameter. Thus mounting a scraper tool against the side of the wheel will produce an additional friction force during icing conditions. As the friction increases, so does the required torque to keep the wheel spinning, and ice can be detected (Jackson and Goldberg, 2007).

3.5 Ultrasonic Guided Waves Sensor

Ultrasonic waves can be used to analyze material properties by sending acoustic waves through the material and recording the resulting ultrasonic response. In the context of aircraft, ultrasonic guided waves can be used to detect changes in an airframe mass and stiffness as a result of ice accretion. This is possible because the recorded response waves have different amplitude and transmission times depending on the presence of ice on the airframe. An implementation of ultrasonic guided waves can be found in (Mendig et al., 2018), where the method is used to detect ice layer thickness and the type of ice accreted on an airfoil. Other ice detection methods based on ultrasonic measurements in the airframe can be found in the following literature (Hongerholt et al., 2001; Liu et al., 2008; Gao and Rose, 2009; Liu et al., 2014; Zhao and Rose, 2016).

3.6 Time Domain Reflectometry Sensors

Time domain reflectometry (TDR) is a technique used to detect changes in the material surrounding an arbitrary surface. The fundamental principle behind TDR is based on the correlation between the propagation velocity of an electromagnetic pulse in a transmission line and the dielectric constant of the surrounding material or substance. Specifically, the dielectric constant of the substance is highly dependent on its water content, which can be used to infer the presence of water and ice. A TDR-based ice detection method developed for aircraft can be found in (Yankielun et al., 2002; Bassey and Simpson, 2007).

3.7 Pitot Tube Based Ice Detection

Pitot tubes are primarily used as airspeed sensors. However, as several research articles show, this pitot tube can also be used for in-flight icing detection. For instance, Hansen and Blanke (2014) use a hypothesis test based on an airspeed observer residual to detect pitot tube clogging. Jackson (2015) proposes to use temperature sensors to monitor and detect ice build-up on the pitot tube, whereas, in (Lv et al., 2020), the change in measured atmospheric pressure is used for ice detection.

3.8 Fiber-optic Ice Detection

An optical ice-detection sensor may use an optical source and a series of optical receivers placed on either side of

the source. In this type of sensor, the amount of light scattering can be analyzed to determine the presence of ice in the path between the optical source and the receivers. Further analysis of the scattered light can be used to determine the thickness and type of ice build-up. Several articles presenting optical-based ice-detection solutions developed for aircraft are listed here (Armstrong et al., 2003; Ikiades, 2007; Ikiades et al., 2007; Li et al., 2009; Braid et al., 2011; Ikiades et al., 2013; Zou et al., 2013; Strobl et al., 2015; Martínez et al., 2017; Prasad et al., 2019; Musci et al., 2020; Gonzalez and Frövel, 2022).

4. ATMOSPHERIC ICING DETECTION

In this section, methods that focus on detecting atmospheric icing conditions, such as supercooled liquid droplets, are presented.

4.1 Weather-radar Based Icing Detection

Weather and cloud monitoring is commonly performed using airborne radar-based techniques, which involve scanning the sky in front of the aircraft to classify the type of clouds that are present. Recent advances in radar technology, coupled with the use of sophisticated data-based classification algorithms, have significantly improved the accuracy and efficacy of this approach. Several papers have been published on weather monitoring ice avoidance techniques, including (Bannister, 2000; Ray et al., 2009; Harrah et al., 2019). The most recent paper on this topic, (Dudek et al., 2021), presents a novel approach that combines weather radar with a visual camera to predict and avoid icing conditions. Specifically, the camera is used to estimate the size and distance of the clouds in the aircraft's path, while weather radar is used to analyze the contents of the clouds and determine the probability of icing conditions.

4.2 Flight Risk Assessment Using Extreme Value Theory

Although not strictly an atmospheric icing detection method, flight risk assessment can be considered an atmospheric sensing method that quantifies risks associated with icing conditions. An example of flight risk assessment can be found in (Pei et al., 2018). The presented method employs an aerodynamic model and an icing effect model to calculate the extreme values of critical flight parameters, such as stall angle, which then serve as stability thresholds for the aircraft. The probabilities of these flight parameters exceeding the maximum value thresholds are subsequently used to estimate the accident probability in various icing scenarios based on atmospheric conditions.

5. INDIRECT PERFORMANCE DEGRADATION DETECTION

A considerable number of methods for in-flight icing detection have been developed using aircraft dynamics modeling. The detection process involves observing aircraft performance degradation and analyzing the performance estimation residuals. The models used in estimation can be categorized into two main groups: motion models and performance models. Motion models describe the aircraft's trajectory, while performance models define the relationship between input throttle and generated acceleration. Furthermore, these models can be augmented with wind models and icing effect models to capture the impact of ice accretion on the aircraft. This section presents all the relevant aircraft motion, performance, and icing models.

5.1 Motion Models

The base case for most aerodynamic motion models is a nonlinear coupled 6-DoF model. However, this base case model is often reduced and simplified to optimize estimation efficiency and convergence. There are two common simplification techniques, one is decoupling into longitudinal and lateral dynamics, and the other one is linearization. Decoupled and linearized models require fewer states, are easier to implement, and can produce good results if the assumptions used to justify the simplification are not violated. Additional simplification can be done by reducing the degrees of freedom, resulting in 2-DoF and 1-DoF models. Most of the aerodynamic models covered in this survey are based on decoupled longitudinal equations of motion given by the following relation:

$$\begin{bmatrix} \dot{u} = rv - qw + \frac{1}{\mathsf{m}}\left(-\mathsf{m}g\sin\theta - D\cos\alpha + L\sin\alpha + \mathrm{T}\right) \\ \dot{w} = qu - pv + \frac{1}{\mathsf{m}}\left(\mathsf{m}g\cos\theta - D\sin\alpha - L\cos\alpha\right) \\ \dot{q} = \frac{1}{I_{yy}}\left(pr\left(I_{zz} - I_{xx}\right) - \left(p^2 - r^2\right)I_{xz} + m_{\mathcal{A}} + m_{\mathrm{T}}\right) \end{bmatrix} \tag{1}$$

where $m_{\mathcal{A}}$ is used as a collective term for aerodynamic pitch moments. An example of a linearized longitudinal 2-DoF model, based on (1), can be found in (Cristofaro and Johansen, 2015), which is also shown below:

$$\begin{aligned} \begin{bmatrix} \dot{V}_a \\ \dot{\alpha} \\ \dot{q} \\ \dot{\theta} \end{bmatrix} &= \begin{bmatrix} X_{V_a} & X_\alpha c_\alpha & X_q & -g\cos\theta_0 \\ \frac{Z_{V_a}}{V_0 c_\alpha} & Z_\alpha & \frac{Z_q}{V_0 c_\alpha} & -\frac{g\sin\theta_0}{V_0 c_\alpha} \\ m_{V_a} & m_\alpha c_\alpha & m_q & 0 \\ 0 & 0 & 1 & 0 \end{bmatrix} \begin{bmatrix} V_a \\ \alpha \\ q \\ \theta \end{bmatrix} \\ &+ \begin{bmatrix} X_{\delta_{th}} & X_{\delta_e} \\ 0 & \frac{Z_{\delta_e}}{V_0 c_\alpha} \\ m_{\delta_{th}} & m_{\delta_e} \\ 0 & 0 \end{bmatrix} \begin{bmatrix} \delta_{th} \\ \delta_e \end{bmatrix} = Ax + Bu \end{aligned} \tag{2}$$

where $c_\alpha := \cos(\alpha_0)$ is defined for conciseness. The states in this linearized state-space formulation are the horizontal airspeed V_a, the angle of attack α, the pitch rate q, and the pitch angle θ. Parameters with subscript 0 indicate chosen trim values for the angle states and the airspeed. The system matrices A, B, used in many of the estimation methods, are formulated using the coefficients in (3),

$$X_\ell = \mu_{X_\ell}\bar{q}C_{X_\ell} \;\;,\;\; Z_\ell = \mu_{Z_\ell}\bar{q}C_{Z_\ell} \;\;,\;\; m_\ell = \frac{\mu_{m_\ell}\bar{q}C_{m_\ell}}{I_{yy}} \tag{3}$$

where C_{*_ℓ} with $\ell \in \{V_a, \alpha, q, \delta_{th}, \delta_e\}$ are nondimensionalized aerodynamic coefficients, $\bar{q}$ is the trimmed dynamic pressure, and μ_* are aircraft specific coefficients based on aircraft geometry.

The nondimensionalized aerodynamic coefficients C_* are generally referred to as static stability and control derivatives, where the "derivate" part comes from the fact that the coefficients originate as partial derivatives in the Taylor series linearization, e.g., $C_{L_\alpha} \triangleq \frac{\partial C_L}{\partial \alpha}$. Identifying and detecting the change in these coefficients is at the root of

many aerodynamic-performance-based ice detection methods. Moreover, identifying stability and control derivatives is essential for calculating the aircraft's stall conditions and other safety margins.

5.2 Icing Effect Models

Most of the reviewed papers in this survey use the icing effect model proposed by Bragg et al. (2000). The idea of the method is to define a model with a base coefficient representing the nominal state and an additive term that incorporates the changes due to icing. For any aerodynamic model coefficient or derivative C_*, the following icing degradation effect model is proposed,

$$C_*^\star = (1 + \eta_{ice} K_{C_*}) C_* \tag{4}$$

where $\eta_{ice}(t)$ is an icing severity coefficient that depends on the icing exposure time t and atmospheric conditions, K_{C_*} is a constant icing factor that is specific to the coefficient being modified, and $C_*^\star$ is an arbitrary aerodynamic coefficient affected by ice accretion. Identifying the nominal and iced coefficients and extracting the icing severity η_{ice} is at the base of many of the performance-based icing detection methods. The subsequent sections present different ways of achieving these tasks.

Besides the Bragg model, other icing effect modeling approaches are:

- The multiplicative method employed by Caliskan,
$$C_*^\star = \eta_{ice} C_*$$
- Icing CFD-based methods that track the liquid droplets and model ice accretion on the particle level, as used by McKillip et al. (2002, 2022).
- A general performance degradation approach, based on energy consideration, where the assumption is that ice leads to decreased aircraft efficiency through increased drag and decreased lift.

5.3 Aircraft Performance Models

In recent papers, a new type of methodology has been presented as a way to detect in-flight icing. The methodology uses a performance reference model to detect degradation and infer ice accretion on the aircraft.

An example is (Coates et al., 2019) and the extended work (Løw-Hansen et al., 2023), where the electric propulsion system of a UAV is modeled such that the difference between the known nominal propeller power and the real-time estimated power can be compared to detect propeller performance degradation and, thereby, ice accretion.

A more comprehensive study using performance monitoring is presented in (Deiler and Fezans, 2020), where an extensive aircraft propulsion model is used for in-flight icing detection. This method is described in greater detail in the following paragraphs.

According to Deiler and Fezans (2020), the aircraft flight performance can be split into the following components:

$$\begin{aligned}\textbf{Flight Performance} &= \text{Nominal Aircraft Performance} \\ &+ \text{Nominal Engine Influence} \\ &+ \text{Variation}\end{aligned}$$

where the "Variation" component includes various performance degrading effects, including in-flight icing. The ice-related degradation can be identified by acquiring the following knowledge. First, it is necessary to know both the nominal and the most extreme variations in flight performance. Then, for the remaining variations in performance, an icing effect model is required.

The aircraft performance is derived based on the time derivative of the total energy of the airplane,

$$\begin{aligned}E_{\text{tot}} &= \frac{1}{2}\mathsf{m}V_a^2 + \mathsf{m}gh \\ \dot{E}_{\text{tot}} &= \mathsf{m}V_a\dot{V}_a + \frac{1}{2}\dot{\mathsf{m}}V_a^2 + \dot{\mathsf{m}}gh + \mathsf{m}g\dot{h}\end{aligned}$$

which combines the aerodynamic influences of wind and potential energy.

The reference power $\dot{E}_{\text{tot,ref}}$ is calculated through a comprehensive performance model, identified using large amounts of real flight data. According to Deiler and Fezans (2020), the high accuracy of the performance model is crucial for the success of their detection method. The performance model is identified by a system identification process where the vector of optimal model parameter values, P_{opt}, is found by minimizing the following error,

$$\mathrm{P}_{\text{opt}} = \text{argmin}_{\mathrm{P}} \left(\dot{E}_{\text{tot,ref(P)}} - \dot{E}_{\text{tot}} \right)^2$$

The difference between the reference power $\dot{E}_{\text{tot,ref}}$, found through offline system identification, and the measured power $\dot{E}_{\text{tot}}$, is used online to find the equivalent change in the drag coefficient,

$$\Delta C_D \approx \frac{\dot{E}_{\text{tot,ref}} - \dot{E}_{\text{tot}}}{V_a \cdot \bar{q} \cdot S} \tag{5}$$

The in-flight icing detection is then made by thresholding the computed drag coefficient delta in (5), where the optimal detection threshold is chosen based on empirical data analysis and is computed as follows:

$$(\Delta C_D)_{\text{crit}} = 30\% C_{D_0}$$

An advantage of the performance-based methods, such as the one described here, is that they do not require additional sensor measurements except for the standard sensor suite, including Global Navigation Satellite System (GNSS), Inertial Measurement Unit (IMU), airspeed, and propulsion system data. Another advantage of these methods is that they do not require dynamic excitation of the aircraft to detect ice accretion on the aircraft. Most observer-based parameter identification algorithms presented in section 6 require excitation of different dynamic modes, which can be unsafe to perform in icing conditions. A drawback of the performance-based methods is their reliance on models that can accurately describe the aircraft dynamics in nominal conditions, which can be challenging to identify without large amounts of data (Deiler and Fezans, 2020).

5.4 Wind Models

In most cases, aircraft have instruments to measure the airspeed V_a, but not the body frame velocity in three dimensions, needed to model the aerodynamic forces experienced by the aircraft. When the wind speed is small

relative to the airspeed, the full velocity vector is not required. However, in many cases, especially involving small fixed-wing UAVs, the wind effect is significant and cannot be overlooked. In such cases, wind models can be used to estimate and decouple wind and aircraft velocities, making it possible to estimate the body frame velocity, angle of attack, and sideslip — states often required to identify aerodynamic coefficients.

Several researchers have used wind models to augment aircraft dynamics in the context of in-flight icing detection. These include simplified wind triangle models and more complex models such as the Dryden wind model (Beard and McLain, 2012, p. 55) that models the unsteady wind components. The use of wind models as part of in-flight icing detection solutions can be found in (Hansen and Blanke, 2014; Wenz and Johansen, 2016, 2019; Deiler and Fezans, 2020).

5.5 Measurement Requirements

Models-based methods rely on sensor data to provide model state information. Moreover, the complexity of the model dictates the quality and type of measurements required to produce accurate prediction results.

When it comes to implementing estimation and detection algorithms, the cost of sensors becomes an issue to be handled. Often inexpensive UAVs do not fly with multihole air probes or vanes, which complicates the parameter identification in icing conditions. The possibility of air data estimation for fixed-wing UAVs without expensive multihole air probes and vanes has been researched by, e.g., Johansen et al. (2015), resulting in the development of methods for estimating wind velocity, angle-of-attack, and sideslip using a standard UAV sensors suite comprising GNSS, IMU, pitot-static tube and barometric altimeter.

To provide an overview of the necessary measurements for the models outlined in this survey, the measurement requirements have been divided into three categories:

- Full-state information, where all system states are assumed available as noisy measurements,
- Standard flight control sensor suite including GNSS, IMU, pitot-static tube, and barometric altimeter.
- Prupolsion system measurements, including data like throttle, motor current, motor shaft speed, and motor temperature.

6. ESTIMATION AND DETECTION METHODS

Since the 1960s, the automatic control research community has developed and refined several model-based estimation methods. Some of these methods have been applied to in-flight icing detection and are therefore briefly explained here. Furthermore, an overview of the models and methods used in each reviewed article on indirect ice detection is presented in Tables 1 and 2.

6.1 Linear Model Estimators

Kalman Filter (KF) is a state estimation algorithm (Brown and Hwang, 2012), which utilizes system dynamics and measurements to make optimal state estimates. In the most simplistic form, the optimality is assured by an adaptive gain referred to as the Kalman gain, which sets the optimal information source ratio for the system's update. If the signal-to-noise is high, measurements are prioritized; otherwise, the system dynamics are prioritized.

The standard KF framework requires a state-space representation of the system, which in the discretized form is given as follows:

$$\begin{aligned} x_k &= A_k x_{k-1} + B_k u_k + \omega_k \\ y_k &= C_k x_k + \upsilon_k \end{aligned} \tag{6}$$

where ω_k and υ_k are the process and measurement noise, respectively. Both ω_k and υ_k are zero mean white Gaussian noise processes with covariance matrices (Q , R):

$$\mathrm{E}\left[\begin{pmatrix} \omega_k \\ \upsilon_k \end{pmatrix} (\omega_k^T \, , \, \upsilon_k^T) \right] = \begin{bmatrix} Q_k & 0 \\ 0 & R_k \end{bmatrix}$$

Given the system model in (6), the KF algorithm can be formulated as shown in (7), where the subscripts indicating the time dependence of the state-space and covariance matrices were dropped for simplicity.

$$\begin{aligned} \hat{x}_{k|k-1} &= A\hat{x}_{k-1} + Bu_k \\ P_{k|k-1} &= AP_{k-1}A^T + Q \\ \mathcal{K}_k &= P_{k|k-1}C^T \left(CP_{k|k-1}C^T + R \right)^{-1} \\ P_k &= \left(I - \mathcal{K}_k C \right) P_{k|k-1} \\ \hat{x}_k &= \underbrace{\hat{x}_{k|k-1}}_{\text{prediction}} + \underbrace{\mathcal{K}_k (y_k - C\hat{x}_{k|k-1})}_{\text{update}} \end{aligned} \tag{7}$$

where $\hat{x}_k$ is the state estimate, $\mathcal{K}_k$ is the Kalman gain and P_k is the error covariance matrix.

The algorithm in (7) has to be initialized with tuning parameters $\mathcal{K}_0$ and P_0. The process noises covariance matrix Q can be based on domain knowledge. Similarly, the measurement noise covariance matrix R can be obtained from the datasheet of the corresponding sensor. If the necessary information is unavailable, the Q and R matrices can be used as tuning parameters.

The use of KF for indirect ice detection can be found in (Johnson and Rokhsaz, 2001; Aykan et al., 2005b), where KF is used for aircraft state estimation to remove measurement noise from the states, which are later fed into a neural network (NN) for detection. Another use case is presented in (Ding et al., 2021), where aerodynamic coefficients are formulated as states in an augmented KF, and the presence of ice is detected based on estimation residuals.

Real-time Parameter Identification (RTPID) is a frequency domain, least squares (LS) regression-based identification algorithm that has been used to estimate aerodynamic coefficients with the goal of detecting ice accretion in (Gingras et al., 2009, 2010). The RTPID algorithm uses state measurements and a deterministic linearized model of the type shown in (6), but with no process noise, in an LS formulation to estimate aerodynamic coefficients.

The estimates are then compared to the nominal a priori coefficients to determine the icing state.

6.2 Nonlinear Filters

Extended Kalman Filter (EKF) is an extension of KF to nonlinear models. This is done through linearization at each iteration of the EKF loop, where the linearization point is based on the previous EKF estimate. Even though EKF works in many situations, the estimated linearization point can be far off during certain scenarios, making other nonlinear methods preferable in those cases. The EKF is used for indirect ice detection in (Aykan et al., 2005a; Caliskan and Hajiyev, 2012; Hajiyev et al., 2005; Hansen and Blanke, 2014; Wenz and Johansen, 2016).

Unscented Kalman Filter (UKF) works by running the prediction and update steps of a regular KF on a group of sample points. Weighted averaging of the sample points allows the UKF to calculate the statistical distribution of the filter states as they undergo nonlinear transformations and measurement updates (Wan and Van Der Merwe, 2000). The UKF has the advantage of allowing nonlinear dynamics in the update step at the cost of an increase in required computational resources. The use of UKF for ice detection is presented in (Wenz and Johansen, 2019).

Fault Detection Filter (FDF), similarly to a KF, is based on estimation residuals. In an FDF, these residuals are fed back through the process model as a weighted sum structured so that it is susceptible to detecting specific pre-defined system faults, e.g., an increase in drag due to ice accretion on the aircraft. In practice, these faults can be caused by sensor offsets, signal drift, or scaling errors, all influencing the observed dynamics of the modeled system.

Implementation of generic FDF can be found in several papers. For example, in (McKillip et al., 2002, 2022), FDF was used for indirect ice detection first on a V-22 Osprey and, more recently, on an eVTOL aircraft.

Bayes Filter (BF) can be viewed as a generalized KF that does not require model states and measurements to have Gaussian distribution. Given the required distribution, the BF can be used to calculate the likelihood of icing state, as it is done by Haaland et al. (2021).

6.3 Unknown Input Observer

Unknown input observer (UIO) is a type of FDF that can be applied to a class of linear time-invariant dynamic systems where the process uncertainty can be modeled as an additive disturbance term $d(t)$, and the other disturbances can be attenuated. If applicable, this allows for the formulation of residuals sensitive to user-defined model uncertainties, such as model-parameter change due to icing. The state space formulation for an UIO can be set up as follows:

$$\begin{aligned} \dot{x}(t) &= Ax(t) + Bu(t) + Ed(t) \\ y(t) &= Cx(t) \end{aligned} \tag{8}$$

where $x(t)$ is the state vector, $y(t)$ is the output vector and $u(t)$, $d(t)$ are known and unknown input vectors respectively. The UIO framework allows one to model parametric uncertainties, nonlinearities, and input noise using the unknown input term $Ed(t)$ and estimate system states despite this unknown input. As described in (Nazari, 2015), when using the UIO, the estimation problem is solved such that the estimation error $e(t) = x(t) - \hat{x}(t)$ asymptotically approaches zero for all $d(t)$. The dynamics of an UIO for the system in (8) are as follows:

$$\begin{aligned} \dot{z}(t) &= Fz(t) + TBu(t) + Ky(t) \\ \hat{x}(t) &= z(t) + Hy(t) \end{aligned}$$

where $\hat{x}$ is the state estimate, z is the full-order dynamic observer state, and F, T, K, H are design matrices used to decouple state estimation dynamics from the disturbance term and produce the necessary conditions for an UIO. Expansion of the error dynamics term $\dot{e}(t)$ shows how such decoupling is possible to achieve.

$$\begin{aligned} \dot{e}(t) = &\left(A - HCA - K_1C\right) e(t) \\ &+ \left[\left(A - HCA - K_1C\right) - F)\right] z(t) \\ &+ \left[\left(A - HCA - K_1C\right)H - K_2\right] y(t) \\ &+ \left[\left(I - HC\right) - T\right] Bu(t) - \left(HC - I\right) Ed(t) \end{aligned}$$

where I is the identity matrix and $K = K_1 + K_2$. To remove the dependencies of $\dot{e}(t)$ on $d(t)$, the design matrices can be chosen as follows,

$$\begin{aligned} F &= A - HCA - K_1C \\ K_2 &= FH \\ T &= I - HC \\ 0 &= \left(HC - I\right) E \end{aligned}$$

resulting in the following decoupled estimation error dynamics necessary for an UIO,

$$\dot{e}(t) = Fe(t)$$

In practice, this means that the estimation error is sensitive only to the change in the system matrices A and B and not to changes in the $d(t)$ signal, thus allowing for residual-based fault detection. Application of UIOs for indirect ice detection can be found in (Tousi and Khorasani, 2009, 2011; Seron et al., 2015; Cristofaro and Johansen, 2015; Rotondo et al., 2018, 2019).

Linear Parameter Varying Estimation (LPV) is a technique that makes it possible to formulate nonlinear dynamics in a linear-like model by incorporating the model's nonlinearities into varying parameters. This way, LPV can enhance estimation methods developed for linear systems, such as UIO, resulting in an estimation method consistent for a larger range of operational modes and trim conditions (Rotondo et al., 2015).

6.4 H_∞ Observer

The H_∞ method augments the standard state-space model in (2) such that the system dynamics become linear in the parameters to be identified, in the following way,

$$\begin{aligned} \dot{x} &= A(x,u)\chi + b(x,u) + d_p \\ \dot{\chi} &= H\chi + Kd_\chi \\ y &= x + d_m \end{aligned} \tag{9}$$

where x is the system state vector, y is the measured output vector, u is the input vector, χ is the parameter

vector, d_p, d_m are the process and measurement noises, d_χ is the model bias, and H, K are constant weights. The particular state-space formulation in (9) is linear in the parameter χ but might include nonlinear terms of x and u in $A(x,u)$ and $b(x,u)$. The advantage of the H_∞ formulation is that it makes it possible to accurately identify time-variant parameters despite unmodeled dynamics, process noise, and measurement noise.

When applying the H_∞ method to indirect ice detection, the parameters to be identified are the stability and control derivatives C_*. Using the nominal and iced parameter definition from (4), such that $\chi_0 = C_*$ and $\chi = C_*^\star$, gives the following χ,

$$\chi = (1 + \eta_{ice} K_{C_*})\chi_0$$

Dynamics of the parameters χ can be defined in several ways depending on the icing scenario. A model used in (Dong and Ai, 2014) is presented here,

$$\dot{\chi} = \chi_0 K_{C_*} N_1 \left(1 + \eta_{ice} N_2\right) \times \left\{ \frac{1}{2}\left[1 - \cos\left(\frac{2\pi t}{T_{cld}}\right)\right] + d_\eta \right\}$$

where the d_η term represents the bias and uncertainty of the model, and N_1, N_2 are constants based on the expected icing severity profile, given by the duration time of the icing encounter T_{cld} and the final and middle values of the icing severity η_{ice} during the icing encounter.

The goal of the H_∞ identification algorithm is to achieve a guaranteed disturbance attenuation level $\gamma^* \leq \gamma$ between the parameter estimation error and the unknown model terms as shown in (10), while also producing converging parameter estimates $\hat{\chi}$. The following inequality describes the disturbance attenuation objective:

$$\begin{aligned} \|\chi - \hat{\chi}\|_Q^2 \leq \gamma^2 \Big[&\left(\|d_p\|_I\right)^2 + \left(\|d_m\|_I\right)^2 + \left(\|d_\chi\|_I\right)^2 \\ &+ \left(\|d_\eta\|_I\right)^2 + \left(|x_0 - \widehat{x}_0|_{P_0}\right)^2 + \left(|\chi - \widehat{\chi}_0|_{Q_0}\right)^2 \Big] \end{aligned} \tag{10}$$

where $\|*\|_Q$ is a weighted L_2 norm, $|*|_{Q_0}$ is a weighted Euclidean norm and $\hat{x}_0$, $\hat{\chi}_0$ are a priori state and parameter estimates. Since the system states are seldom available, the practical formulation requires estimating the states as part of the problem. Recent applications of H_∞ identification algorithm for in-flight icing detection can be found in (Schuchard et al., 2000; Melody et al., 2000, 2001; Ying et al., 2013; Dong and Ai, 2013).

6.5 Moving Horizon Estimation

A moving horizon estimator (MHE) is a flexible state estimation framework that combines model equations with sensor measurements from a fixed time window. The estimation problem is solved as an optimization problem by minimizing the model prediction error in the specified time window. The MHE framework is highly flexible regarding model size and complexity. However, the increased computational complexity associated with large and nonlinear models might reduce the applicability of the MHE in

Table 1. Part 1. Overview of articles on indirect ice detection.

		Estimation Method (sections 6.1.1 and 6.2 to 6.6)				**Model and States (section 5.1)**		
	Paper	**KF**	**UIO**	**H_∞**	**FDF**	**Linear**	**Nonlinear**	**Propulsion System**
1	Johnson and Rokhsaz (2001)	KF				u,α,q,θ		
2	Aykan et al. (2005b)	KF				u,α,β,p,q,r,ϕ,θ,ψ		
3	Caliskan and Hajiyev (2012)	EKF				u,α,β,p,q,r,ϕ,θ,ψ		
4	Cristofaro et al. (2017)	MME (KF)				u,v,w,p,q,r,ϕ,θ,ψ		
5	Cristofaro et al. (2015)	MME (KF)				V_a, α,q,θ		
6	Haaland et al. (2021)	MME (KF)						V_a, ω, i
7	Rotondo et al. (2017)	MME LPV					u,w,q, θ	
8	Aykan et al. (2005a)	EKF				u,α,β,p,q,r,ϕ,θ,ψ		
9	Caliskan et al. (2008)	EKF				u,α,β,p,q,r,ϕ,θ,ψ		
10	Hajiyev et al. (2005)	EKF				u,α,β,p,q,r,ϕ,θ,ψ		
11	Rotondo et al. (2015)		LPV UIO				u,w,q, θ	
12	Rotondo et al. (2018)		LPV UIO				u,v,w,p,q,r,ϕ,θ,ψ,h	
13	Rotondo et al. (2019)		LPV integral UIO				u,w,q, θ	
14	Seron et al. (2015)		MME UIO			u,w,q,θ		
15	Tousi and Khorasani (2011)		UIO			v,β,p,r,ϕ,ψ		
16	Tousi and Khorasani (2009)		UIO			v,β,p,r,ϕ,ψ		
17	Cristofaro and Johansen (2015)		UIO			V_a, α,q,θ		
18	Melody et al. (2000, 2001)			**H_∞**			u,w,α,q,q,θ,C_*{9} *	
19	Dong and Ai (2013, 2014)			**H_∞**			u,v,w,p,q,r,ϕ,θ,ψ,C_*{6}	
20	Schuchard et al. (2000)			**H_∞**			u,α,q,θ,C_*{9}	
21	Ying et al. (2013)			**H_∞**			u,α,q,θ,C_*{9}	
22	Miller and Larsen (2003)				FDF	u,α,q,θ		
23	McKillip et al. (2002)				FDF			T,Q,ω
24	McKillip et al. (2022)				FDF			T,Q,ω
25	Ding et al. (2021)	UKF				V_a,α,q,θ,h,C_*(5)		
26	Deiler and Fezans (2020)							×
27	Hansen and Blanke (2014)	EKF	Velocity observer			V_w,ψ_w,λ	V_a,C_{X_0}, C_{X_α}	
28	Wenz and Johansen (2016)	EKF				V_{sw},V_{dw},C_{L_0},C_{L_α},λ		
29	Wenz and Johansen (2019)	MSE (UKF) **					V_{sw},V_{dw},C_{L_0},C_{L_α},λ	
30	Ding et al. (2020)					V_a, α,q,θ,h		
31	Gingras et al. (2009, 2010)					u,α,β,p,q,r,h		
32	Coates et al. (2019)							T,Q,ω
33	Baskaya et al. (2017)							
34	Dong (2018, 2019)						u,v,w,p,q,r,ϕ,θ,ψ	
35	Sørensen et al. (2015)						u,v,w,p,q,r,ϕ,θ,ψ	

* 9 aerodynamic coefficients

** Nonlinear optimization method where UKF is used to provide the state covariance matrix

Table 2. Part 2. Overview of articles on indirect ice detection.

		Detection Method and Decision Variables (sections 6.6 to 6.8)				**Icing Model (sections 5.2 to 5.4)**			**Measurements (section 5.5)**			
	Paper	Threshold	MME	GLRT	NN	Bragg	Performance Degradation	Multiplicative	Full-state Information	Standard	Propulsion System	**Aircraft**
1	Johnson and Rokhsaz (2001)				ANN, KF states, δ_{th}		×		×			DHC-6 Twin Otter
2	Aykan et al. (2005b)	ANN output		KF residuals	ANN, KF states			×	×			A340
3	Caliskan and Hajiyev (2012)	ANN output		KF residuals	ANN, KF states			×	×			A340
4	Cristofaro et al. (2017)		KF states			×			×	×		Aerosonde UAV
5	Cristofaro et al. (2015)		KF states			×			×	×		Aerosonde UAV
6	Haaland et al. (2021)		BF Hyptheses				×		×			Skywalker X8
7	Rotondo et al. (2017)		KF states			×			×			DHC-6 Twin Otter
8	Aykan et al. (2005a)	ANN output		EKF residuals	ANN, EKF states			×	×			F16, A340
9	Caliskan et al. (2008)	ANN output		EKF residuals	ANN, EKF states			×	×			F16, A340
10	Hajiyev et al. (2005)	ANN output		EKF residuals	ANN, EKF states			×	×			F16
11	Rotondo et al. (2015)	UIO residuals				×			×	×		Zagi UAV
12	Rotondo et al. (2018)	UIO residuals				×			×	×		DHC-6 Twin Otter
13	Rotondo et al. (2019)	UIO residuals				×			×	×		Zagi UAV DHC-6 Twin Otter
14	Seron et al. (2015)		η_{ice} (UIO residual)			×			×	×		Aerosonde UAV
15	Tousi and Khorasani (2011)			UIO residuals		×			×			DHC-6 Twin Otter
16	Tousi and Khorasani (2009)			UIO residuals		×			×			AeroSim Aerosonde
17	Cristofaro and Johansen (2015)	UIO residuals				×			×	×		Aerosonde UAV
18	Melody et al. (2000, 2001)	C_{m_α}, $C_{m_{\delta_e}}$, C_{m_q}				×			×			DHC-6 Twin Otter
19	Dong and Ai (2013, 2014)				PNN, (C_{l_p},$C_{l_{\delta_a}}$, C_{m_α},$C_{m_{\delta_e}}$,C_{n_β},$C_{n_{\delta_a}}$)		×					DHC-6 Twin Otter
20	Schuchard et al. (2000)	η_{ice}			ANN, C_{m_α}, $C_{m_{\delta_e}}$	×			×			DHC-6 Twin Otter
21	Ying et al. (2013)	η_{ice}			ANN, C_{m_α}, $C_{m_{\delta_e}}$, C_{m_q}	×			×			DHC-6 Twin Otter
22	Miller and Larsen (2003)			Observer residuals		×			×			DHC-6 Twin Otter
23	McKillip et al. (2002)	Observer residuals					×			×	×	V22 osprey
24	McKillip et al. (2022)	Observer residuals					×			×	×	Elroy air Chaparral UAS
25	Ding et al. (2021)	η_{ice}(C_{L_α},$C_{L_{\delta_e}}$, C_{m_α},C_{m_q},$C_{m_{\delta_e}}$)				×			×			A340 (shape)
26	Deiler and Fezans (2020)	C_D, C_L				×				×	×	A320
27	Hansen and Blanke (2014)			V_w, V_a,T			×			×		Banshee UAV
28	Wenz and Johansen (2016)	C_{L_0},C_{L_α},α,V_a					×			×		Skywalker X8 UAV
29	Wenz and Johansen (2019)	C_{L_0},C_{L_α},α,V_a					×			×		Skywalker X8 UAV
30	Ding et al. (2020)			C_X C_Z, q		×			×	×		A340 (shape)
31	Gingras et al. (2009, 2010)	C_{m_α}, $C_{m_{\delta_e}}$, C_{N_α}, C_{l_β},$C_{l_{\delta_a}}$					×			×		DHC-6 Twin Otter
32	Coates et al. (2019)	C_D					×				×	Skywalker X8 UAV
33	Baskaya et al. (2017)				SVM *, Gyro , IMU, δ_{th}		× **			×		MAKO UAV
34	Dong (2018, 2019)				RNN,DNN,TL *** , h, V_a, IMU,p,q,r,ϕ,θ,ψ	×			×	×		DHC-6 Twin Otter
35	Sørensen et al. (2015)			C_X C_Z			×			×	×	Zagi UAV

* support vector machine (SVM)
** Actuator fault
*** transfer learning (TL)

certain applications. An in-depth explanation of the MHE method can be found in (Robertson et al., 1996) and (Wenz and Johansen, 2019), where it is used for in-flight icing detection on UAVs.

6.6 Multiple Model Estimation and Detection

Multiple model estimation (MME) is a framework used for state estimation in the presence of parametric uncertainty by running several estimation filters based on different models and in real-time comparing their likelihood given the measured data. This approach allows one to cover a large set of admissible model parameter values at the expense of computational power. Furthermore, the MME can be easily used in a detection scheme that relies on identifying the model closest to the true system among all concurrently run models, thereby identifying the most likely model. The use of MME for indirect ice detection can be found in the following papers (Cristofaro et al., 2015, 2017; Rotondo et al., 2017; Haaland et al., 2021).

6.7 Neural Networks

The methods for detecting in-flight icing that have been described so far rely on aerodynamic models that are based on physics-based first principles. While this approach can produce reliable results, it is limited by the complexity of the modeled dynamics and the aircraft's operating conditions. In addition, if too many assumptions and simplifications are made, the predictive ability of these models can decrease significantly. To address this limitation, an alternative approach is to use machine learning and artificial neural networks (ANNs) to estimate the states of a dynamical system. The idea behind NNs is to leverage the information hidden in large quantities of sensor and actuator data to learn the system dynamics directly instead of modeling them. NN-based solutions are also highly flexible, allowing the construction of models that can, for example, take IMU measurements as input and output the icing state of the aircraft. The use of ANNs for indirect ice detection on aircraft can be found in the following papers: (Baskaya et al., 2017; Dong, 2018, 2019). An in-depth explanation of ANNs, including deep, recurrent, and probabilistic NNs, (DNN),(RNN), and (PNN), respectively, can be found in (Goodfellow et al., 2017).

6.8 Generalized Likelihood Ratio Test

Hypothesis testing is a method of statistical inference used to decide whether available measurements from a system are sufficiently likely to agree with a particular model describing the system, for instance, whether it operates nominally or experiences performance degradation due to ice accretion on the aircraft. In the hypothesis testing approach, the likelihood of measured data is used to determine if the reference system complies with the proposed hypothesis. Specific applications of hypothesis testing for in-flight icing detection can be found in the following papers: (Miller and Larsen, 2003; Sørensen et al., 2015; Ding et al., 2020).

7. SUMMARY AND CONCLUSION

For conventional aircraft, the challenges associated with in-flight icing are, in general, considered to be solved. However, for smaller fixed-wing UAVs, the available solutions are not directly applicable due to cost, efficiency, and weight limitations.

Several performance-degradation-based ice detection methods have been surveyed and presented in this paper; their strengths and weaknesses can be summarized as follows. Performance-degradation-based methods require precise propulsion systems models; if such models are available, estimation filters and observers can be used to accurately detect ice without the need for additional sensors, except for the standard flight controller sensor suite expected to be present on a UAV. Neural-network-based methods can yield good results and are very flexible in terms of detection problem formulation. However, they require large amounts of labeled data, which can be challenging to acquire. On the other hand, methods such as UKF, MHE, and MME use additional computational resources to compute estimates, making them a suitable option for ice detection if sufficient computation power is available.

Nevertheless, a common limitation of the surveyed papers is that practically none of the performance-based detection methods have been validated in actual flight experiments. In most papers, the methods are validated in simulation, either using simulated data or, in many cases, using NASA's dataset collected with the DHC-6 Twin Otter research aircraft, where (Hansen and Blanke, 2014) stands out as one of the papers presenting flight experiment results. Comparison and validation of the various performance-based ice detection methods in flight experiments is therefore identified as highly beneficial for the further development of ice detection systems.

Furthermore, the research on atmospheric icing and direct ice detection indicates that performance-based methods are not the only solution, and research on ice sensors with a small footprint and low energy requirements shouldn't be overlooked. The same can be said for weather-radar-based solutions, which can be especially relevant for highly trafficked locations with dense traffic, such as urban airports and landing pads where the number of users could justify investment in expensive radar equipment.

REFERENCES

Armstrong, D.J., Hare, G.G., Kloeppel, V., Lawrence, M., Dalton, T., Konstantaki, M., and Ikiades, A. (2003). Air conformal ice detection system (ACIDS) for the power optimised, ice protected aircraft/rotorcraft. Technical report, SAE Technical Paper.

Aykan, R., Hadjiyev, C., and Caliskan, F. (2005a). Aircraft icing detection, identification and reconfigurable control based on kalman filtering and neural networks. In *AIAA Atmospheric Flight Mechanics Conference and Exhibit*, 6220.

Aykan, R., Hajiyev, C., and Çalişkan, F. (2005b). Kalman filter and neural network-based icing identification applied to A340 aircraft dynamics. *Aircraft Engineering and Aerospace Technology*.

Bannister, M. (2000). Drag and dirt deposition mechanisms of external rear view mirrors and techniques used for optimisation. Technical report, SAE Technical Paper.

Baskaya, E., Bronz, M., and Delahaye, D. (2017). Fault detection & diagnosis for small UAVs via machine

learning. In *AIAA/IEEE Digital Avionics Systems Conference - Proceedings*, volume 2017-Septe. Institute of Electrical and Electronics Engineers Inc.

Bassey, C.E. and Simpson, G.R. (2007). Aircraft ice detection using time domain reflectometry with coplanar sensors. In *IEEE Aerospace Conference Proceedings*.

Beard, R.W. and McLain, T.W. (2012). *Small unmanned aircraft: Theory and practice*. Princeton university press.

Botura, G. and Fahrner, A. (2003). Icing detection system - conception, development, testing and applicability to UAVS. In *2nd AIAA "Unmanned Unlimited" Conference and Workshop and Exhibit*. American Institute of Aeronautics and Astronautics Inc.

Bragg, M., Hutchison, T., and Merret, J. (2000). Effect of ice accretion on aircraft flight dynamics. In *38th Aerospace Sciences Meeting and Exhibit*, 360.

Braid, J., Van Wie, P., and Rex, J. (2011). Using the TAMDAR sensor for in-flight ice detection and improved safety of flight. Technical report, SAE Technical Paper.

Brown, R.G. and Hwang, P.Y. (2012). *Introduction to Random Signals and Applied Kalman Filtering with Matlab Exercises*. Wiley.

Caliskan, F., Aykan, R., and Hajiyev, C. (2008). Aircraft icing detection, identification, and reconfigurable control based on kalman filtering and neural networks. *Journal of Aerospace Engineering*, 21(2), 51–60.

Caliskan, F. and Hajiyev, C. (2012). In-flight detection and identification and accommodation of aircraft icing. In *AIP conference proceedings*, volume 1493, 200–206. American Institute of Physics.

Caliskan, F. and Hajiyev, C. (2013). A review of in-flight detection and identification of aircraft icing and reconfigurable control.

Coates, E.M., Wenz, A., Gryte, K., and Johansen, T.A. (2019). Propulsion system modeling for small fixed-wing UAVs. In *2019 International Conference on Unmanned Aircraft Systems, ICUAS 2019*, 748–757. Institute of Electrical and Electronics Engineers Inc.

Cristofaro, A. and Johansen, T.A. (2015). An unknown input observer approach to icing detection for unmanned aerial vehicles with linearized longitudinal motion. In *Proceedings of the American Control Conference*, volume 2015-July, 207–213. Institute of Electrical and Electronics Engineers Inc.

Cristofaro, A., Johansen, T.A., and Aguiar, A.P. (2015). Icing detection and identification for unmanned aerial vehicles: Multiple model adaptive estimation. In *2015 European Control Conference, ECC 2015*, 1651–1656. Institute of Electrical and Electronics Engineers Inc.

Cristofaro, A., Johansen, T.A., and Aguiar, A.P. (2017). Icing detection and identification for unmanned aerial vehicles using adaptive nested multiple models. *International Journal of Adaptive Control and Signal Processing*, 31(11), 1584–1607.

Deiler, C. and Fezans, N. (2020). Performance-based ice detection methodology. *Journal of Aircraft*, 57(2), 209–223.

Ding, D., Qian, W.Q., and Wang, Q. (2020). Aircraft inflight icing detection based on statistical decision theory. In *IOP Conference Series: Materials Science and Engineering*, volume 751, 012054. IOP Publishing.

Ding, D., Qian, W.Q., and Wang, Q. (2021). Aircraft wing ice online detection and fault-tolerant control law design. In *2021 China Automation Congress (CAC)*, 2520–2525. IEEE.

Dong, Y. (2018). An application of Deep Neural Networks to the in-flight parameter identification for detection and characterization of aircraft icing. *Aerospace Science and Technology*, 77, 34–49.

Dong, Y. (2019). Implementing deep learning for comprehensive aircraft icing and actuator/sensor fault detection/identification. *Engineering Applications of Artificial Intelligence*, 83, 28–44.

Dong, Y. and Ai, J. (2013). Research on inflight parameter identification and icing location detection of the aircraft. *Aerospace Science and Technology*, 29(1), 305–312.

Dong, Y. and Ai, J. (2014). Inflight parameter identification and icing location detection of the aircraft: the time-varying case. *Journal of Control Science and Engineering*, 2014.

Dudek, A., Kunstmann, F., Stutz, P., and Hennig, J. (2021). Detect and avoid of weather phenomena onboard UAV: Increasing detection capabilities by information fusion. In *AIAA/IEEE Digital Avionics Systems Conference - Proceedings*, volume 2021-Octob. Institute of Electrical and Electronics Engineers Inc.

Federal Aviation Administration (2022). FAA national forecast 2022-2042. Report, USA.

Fuleki, D., Sun, Z., Wu, J., and Miller, G. (2017). Development of a non-intrusive ultrasound ice accretion sensor to detect and quantify ice accretion severity. In *9th AIAA Atmospheric and Space Environments Conference*, 4247.

Gao, H. and Rose, J.L. (2009). Ice detection and classification on an aircraft wing with ultrasonic shear horizontal guided waves. *IEEE transactions on ultrasonics, ferroelectrics, and frequency control*, 56(2), 334–344.

Gingras, D.R., Barnhart, B., Ranaudo, R., Martos, B., Ratvasky, T.P., and Morelli, E. (2010). Development and implementation of a model-driven envelope protection system for in-flight ice contamination. *AIAA Guidance, Navigation, and Control Conference*.

Gingras, D.R., Barnhart, B., Ranaudo, R., Ratvasky, T.P., and Morelli, E. (2009). Envelope protection for in-flight ice contamination. *47th AIAA Aerospace Sciences Meeting including the New Horizons Forum and Aerospace Exposition*.

Gonzalez, M. and Frövel, M. (2022). Fiber bragg grating sensors ice detection: Methodologies and performance. *Sensors and Actuators A: Physical*, 346, 113778.

Goodfellow, I., Bengio, Y., and Courville, A. (2017). Deep learning (adaptive computation and machine learning series). *Cambridge Massachusetts*, 321–359.

Haaland, O.M., Wenz, A.W., Gryte, K., Hann, R., and Johansen, T.A. (2021). Detection and isolation of propeller icing and electric propulsion system faults in fixed-wing UAVs. In *2021 International Conference on Unmanned Aircraft Systems, ICUAS 2021*, 377–386. Institute of Electrical and Electronics Engineers Inc.

Hajiyev, C., Caliskan, F., and Aykan, R. (2005). EKF and neural network based aircraft icing detection and identification applied to F-16 flight dynamics. In *Proceedings of the European conference for aerospace sciences (EUCASS)*, 4–7.

Hann, R., Borup, K.T., Zolich, A.P., Sørensen, K.L., Vestad, H.N., Steinert, M., and Johansen, T.A. (2019). Experimental investigations of an icing protection system for UAVs. Technical report, SAE Technical Paper.

Hann, R. and Johansen, T.A. (2020). Unsettled topics in unmanned aerial vehicle icing. Technical report, SAE Technical Paper.

Hann, R. and Johansen, T.A. (2021). UAV icing: The influence of airspeed and chord length on performance degradation. *Aircraft Engineering and Aerospace Technology*.

Hansen, S. and Blanke, M. (2014). Diagnosis of airspeed measurement faults for unmanned aerial vehicles. *IEEE Transactions on Aerospace and Electronic Systems*, 50(1), 224–239.

Harrah, S.D., Strickland, J.K., Hunt, P.J., Proctor, F.H., Switzer, G.F., Ratvasky, T.P., Strapp, J.W., Lilie, L., and Dumont, C. (2019). Radar detection of high concentrations of ice particles-methodology and preliminary flight test results. Technical report, NASA.

Hongerholt, D.D., Willms, G., and Rose, J.L. (2001). Ultrasonic in-flight wing ice detection. In *SAE Advances in Aviation Safety Conference-2001 Aerospace Congress*.

Ikiades, A., Howard, G., Armstrong, D.J., Konstantaki, M., and Crossley, S. (2007). Measurement of optical diffusion properties of ice for direct detection ice accretion sensors. *Sensors and Actuators A: physical*, 140(1), 24–31.

Ikiades, A.A., Spasopoulos, D., Amoiropoulos, K., Richards, T., Howard, G., and Pfeil, M. (2013). Detection and rate of growth of ice on aerodynamic surfaces using its optical characteristics. *Aircraft Engineering and Aerospace Technology*.

Ikiades, A.A. (2007). Direct ice detection based on fiber optic sensor architecture. *Applied Physics Letters*, 91(10), 104.

Jackson, D.G. and Goldberg, J.I. (2007). Ice detection systems: A historical perspective. In *SAE Technical Papers*. SAE International.

Jackson, D.A. (2015). Concept of a pitot tube able to detect blockage by ice, volcanic ash, sand and insects, and to clear the tube. *Photonic Sensors*, 5(4), 298–303.

Jarvinen, P. (2007). Aircraft ice detection method. In *45th AIAA Aerospace Sciences Meeting and Exhibit*, 696.

Johansen, T.A., Cristofaro, A., Sørensen, K., Hansen, J.M., and Fossen, T.I. (2015). On estimation of wind velocity, angle-of-attack and sideslip angle of small UAVs using standard sensors. In *2015 International Conference on Unmanned Aircraft Systems*, 510–519. IEEE.

Johnson, M.D. and Rokhsaz, K. (2001). Using artificial neural networks and self-organizing maps for detection of airframe icing. *Journal of Aircraft*, 38(2), 224–230.

Li, W., Zhang, J., Ye, L., and Zhang, H. (2009). A fiber-optic solution to aircraft icing detection and measurement problem. In *2009 International Conference on Information Technology and Computer Science*, volume 1, 357–360. IEEE.

Liu, Q., Wu, K., Kobayashi, M., Jen, C., and Mrad, N. (2008). In situ ice and structure thickness monitoring using integrated and flexible ultrasonic transducers. *Smart materials and structures*, 17(4), 045023.

Liu, Y., Chen, W., Bond, L.J., and Hu, H. (2014). A feasibility study to identify ice types by measuring attenuation of ultrasonic waves for aircraft icing detection. In *Fluids Engineering Division Summer Meeting*, volume 46223, V01BT22A003. American Society of Mechanical Engineers.

Lv, X., Guan, J., Wang, S., Zhang, H., Xue, S., Tang, Q., and He, Y. (2020). Pitot tube-based icing detection: Effect of ice blocking on pressure. *International Journal of Aerospace Engineering*, 2020.

Løw-Hansen, B., Coates, E.M.L., Müller, N.C., Johansen, T.A., and Hann, R. (2023). Identification of an electric UAV Propulsion System in Icing Conditions. Technical report, SAE Technical Paper, (submitted).

Mäder, T., Nestler, M., Kranz, B., and Drossel, W.G. (2018). Studies on sheet-metal compounds with piezoceramic modules for icing detection and de-icing. *Advanced Engineering Materials*, 20(12), 1800589.

Markets and Markets (2018). Military drones market by type, application (ISRT, delivery and transportation, combat operations, battle damage management), range (VLOS, EVLOS, BLOS), propulsion type, launching mode, endurance, MTOW, region - global forecast to 2025. Market Report, retrieved November 2019.

Martín-Martín, A., Thelwall, M., Orduna-Malea, E., and Delgado López-Cózar, E. (2021). Google Scholar, Microsoft Academic, Scopus, Dimensions, Web of Science, and OpenCitations' COCI: a multidisciplinary comparison of coverage via citations. *Scientometrics*, 126(1), 871–906.

Martínez, J., Ródenas, A., Stake, A., Traveria, M., Aguiló, M., Solis, J., Osellame, R., Tanaka, T., Berton, B., Kimura, S., et al. (2017). Harsh-environment-resistant OH-vibrations-sensitive mid-infrared water-ice photonic sensor. *Advanced Materials Technologies*, 2(8), 1700085.

McKillip, R., Kaufman, A., Quackenbush, T., Danilov, P., and Yu, M. (2022). Algorithmic icing detection for eVTOL/AAM aircraft. *AIAA AVIATION 2022 Forum*.

McKillip, R., Keller, J., and Kaufman, A. (2002). Algorithmic icing detection for the V-22 osprey. In *Proc. AHS Flight Controls and Crew Systems Specialists' Meeting, Philadelphia, PA*.

Melody, J.W., Başar, T., Perkins, W.R., and Voulgaris, P.G. (2000). Parameter identification for inflight detection and characterization of aircraft icing. *Control Engineering Practice*, 8(9), 985–1001.

Melody, J.W., Hillbrand, T., Başar, T., and Perkins, W.R. (2001). H_∞ parameter identification for inflight detection of aircraft icing: The time-varying case. *Control Engineering Practice*, 9(12), 1327–1335.

Mendig, C., Riemenschneider, J., Monner, H.P., Vier, L.J., Endres, M., and Sommerwerk, H. (2018). Ice detection by ultrasonic guided waves. *CEAS Aeronautical Journal*, 9(3), 405–415.

Miller, R.H. and Larsen, M.L. (2003). Optimal fault detection and isolation filters for flight vehicle performance monitoring. In *IEEE Aerospace Conference Proceedings*, volume 7, 3197–3203.

Musci, M.A., Mazzara, L., and Lingua, A.M. (2020). Ice detection on aircraft surface using machine learning approaches based on hyperspectral and multispectral images. *Drones*, 4(3), 1–26.

Nazari, S. (2015). The unknown input observer and its advantages with examples. *arXiv preprint arXiv:1504.07300*.

Pei, B., Xu, H., Xue, Y., Chen, W., and Shen, A. (2018). In-flight icing risk prediction and management in consideration of wing stall. *Aircraft Engineering and Aerospace Technology*, 90(1), 24–32.

Prasad, S.B., Hegde, G., and Asokan, S. (2019). Fiber bragg grating based ice detection sensor. In *2019 Workshop on Recent Advances in Photonics (WRAP)*, 1–4. IEEE.

Ray, M., Nesnidal, M., and Socha, D. (2009). Optical detection of airborne ice crystals and liquid water droplets. In *1st AIAA Atmospheric and Space Environments Conference*, 3863.

Robertson, D.G., Lee, J.H., and Rawlings, J.B. (1996). A moving horizon-based approach for least-squares estimation. *AIChE Journal*, 42(8), 2209–2224.

Rotondo, D., Cristofaro, A., Hassani, V., and Johansen, T.A. (2017). Icing diagnosis in unmanned aerial vehicles using an LPV multiple model estimator. In *IFAC-PapersOnLine*, volume 50, 5238–5243. Elsevier.

Rotondo, D., Cristofaro, A., Johansen, T.A., Nejjari, F., and Puig, V. (2015). Icing detection in unmanned aerial vehicles with longitudinal motion using an LPV unknown input observer. *2015 IEEE Conference on Control and Applications, Proceedings*, 984–989.

Rotondo, D., Cristofaro, A., Johansen, T.A., Nejjari, F., and Puig, V. (2018). Diagnosis of icing and actuator faults in UAVs using LPV unknown input observers. *Journal of Intelligent and Robotic Systems: Theory and Applications*, 91(3-4), 651–665.

Rotondo, D., Cristofaro, A., Johansen, T.A., Nejjari, F., and Puig, V. (2019). Robust fault and icing diagnosis in unmanned aerial vehicles using LPV interval observers. *International Journal of Robust and Nonlinear Control*, 29(16), 5456–5480.

Roy, S., De Anna, R.G., Mehregani, M., and Zakar, E. (2000). A capacitive ice detection microsensor. *Sens. Mater*, 12(1), 1–14.

Schlegl, T., Moser, M., Loss, T., and Unger, T. (2019). A Smart Icing Detection System for Any Location on the Outer Aircraft Surface. In *SAE Technical Papers*, volume 2019-June. SAE International.

Schlegl, T., Moser, M., and Zangl, H. (2015). Wireless and flexible ice detection on aircraft. Technical report, SAE Technical Paper.

Schuchard, E., Melody, J., Basar, T., Perkins, W., and Voulgaris, P. (2000). Detection and classification of aircraft icing using neural networks. In *38th Aerospace Sciences Meeting and Exhibit*, 361.

Seron, M.M., Johansen, T.A., De Doná, J.A., and Cristofaro, A. (2015). Detection and estimation of icing in unmanned aerial vehicles using a bank of unknown input observers. In *2015 Australian Control Conference, AUCC 2015*, 87–92. Institute of Electrical and Electronics Engineers Inc.

Sohail, M., Pfeiffer, H., and Wevers, M. (2022). Addressing safety concerns in hybrid electric aircrafts: In-flight icing detection, moisture detection in fuselage and electrical wiring and interconnect system (EWIS). In *IOP Conference Series: Materials Science and Engineering*, volume 1226, 012060. IOP Publishing.

Sørensen, K.L., Blanks, M., and Johansen, T.A. (2015). Diagnosis of wing icing through lift and drag coefficient change detection for small unmanned aircraft. In *IFAC-PapersOnLine*, volume 28, 541–546.

Strobl, T., Adam, R., Entz, R., and Hornung, M. (2015). A hybrid system for ice protection and detection. In *preparation)," International Conference on More Electric Aircraft (MEA2015)*.

Sørensen, K.L. and Johansen, T.A. (2017). Flight test results for autonomous icing protection solution for small unmanned aircraft. In *2017 International Conference on Unmanned Aircraft Systems (ICUAS)*, 971–980.

Tousi, M.M. and Khorasani, K. (2009). Fault diagnosis and recovery from structural failures (icing) in unmanned aerial vehicles. In *2009 IEEE International Systems Conference Proceedings*, 302–307.

Tousi, M.M. and Khorasani, K. (2011). Robust observer-based fault diagnosis for an unmanned aerial vehicle. In *2011 IEEE International Systems Conference, SysCon 2011 - Proceedings*, 428–434.

Wan, E.A. and Van Der Merwe, R. (2000). The unscented kalman filter for nonlinear estimation. In *Proceedings of the IEEE 2000 Adaptive Systems for Signal Processing, Communications, and Control Symposium (Cat. No. 00EX373)*, 153–158. IEEE.

Wenz, A. and Johansen, T.A. (2016). Icing detection for small fixed wing UAVs using inflight aerodynamic coefficient estimation. In *2016 IEEE Conference on Control Applications*, 230–236. Institute of Electrical and Electronics Engineers Inc.

Wenz, A. and Johansen, T.A. (2019). Icing detection for small fixed-wing UAVs using inflight aerodynamic coefficient estimation. In *IEEE Aerospace Conference Proceedings*. IEEE Computer Society.

Xie, J., Wen, J., Chen, J., and Yuan, W. (2022a). Microwave icing sensor based on interdigital-complementary split-ring resonator. *IEEE Sensors Journal*.

Xie, L., Liang, H., Zong, H., Liu, X., and Li, Y. (2022b). Multipurpose distributed dielectric-barrier-discharge plasma actuation: Icing sensing, anti-icing, and flow control in one. *Physics of Fluids*, 34(7), 071701.

Yankielun, N.E., Ryerson, C.C., and Jones, S.L. (2002). Wide-area ice detection using time domain reflectometry. Technical report, US Army Corps of Engineers, Engineer Research and Development Center.

Ying, S.b., Ge, T., and Ai, J.l. (2013). H_∞ parameter identification and H2 feedback control synthesizing for inflight aircraft icing. *Journal of Shanghai Jiaotong University (Science)*, 18(3), 317–325.

Zhao, X. and Rose, J.L. (2016). Ultrasonic guided wave tomography for ice detection. *Ultrasonics*, 67, 212–219.

Zheng, D., Li, Z., Du, Z., Ma, Y., Zhang, L., Du, C., Li, Z., Cui, L., Zhang, L., Xuan, X., et al. (2022). Design of capacitance and impedance dual-parameters planar electrode sensor for thin ice detection of aircraft wings. *IEEE Sensors Journal*, 22(11), 11006–11015.

Zou, J., Ye, L., and Ge, J. (2013). Ice type detection using an oblique end-face fibre-optic technique. *Measurement Science and Technology*, 24(3), 035201.